https://doi.org/10.5194/tc-2020-186
Preprint. Discussion started: 4 August 2020

The Cryosphere Discussions

The tipping points and early-warning indicators for Pine Island Glacier, West Antarctica

Sebastian H. R. Rosier[1*], Ronja Reese[2], Jonathan F. Donges[2,3], Jan De Rydt[1], G. Hilmar Gudmundsson[1], Ricarda Winkelmann[2,4]

[1]Department of Geography and Environmental Sciences, Northumbria University, Newcastle, UK
[2]Earth System Analysis, Potsdam Institute for Climate Impact Research (PIK), Member of the Leibniz Association, P.O. Box 60 12 03, 14412 Potsdam, Germany
[3]Stockholm Resilience Centre, Stockholm University, Kräftriket 2B, SE-10691 Stockholm, Sweden
[4]University of Potsdam, Institute of Physics and Astronomy, Karl-Liebknecht-Str. 24–25, 14476 Potsdam, Germany

Correspondence to: Sebastian Rosier (Sebastian.rosier@northumbria.ac.uk)

Abstract. Mass loss from the Antarctic Ice Sheet is the main source of uncertainty in projections of future sea-level rise, with important implications for coastal regions worldwide. Central to this is the marine ice sheet instability: once a critical threshold, or tipping point, is crossed, ice-internal dynamics can drive a self-amplifying retreat committing a glacier to irreversible, rapid and substantial ice loss. This process might have already been triggered in the Amundsen Sea region, where Pine Island and Thwaites glaciers dominate the current mass loss from Antarctica, but modelling and observational techniques have not been able to establish this rigorously, leading to divergent views on the future mass loss of the WAIS. Here, we aim at closing this knowledge gap by conducting a systematic investigation of the stability regime of Pine Island Glacier. To this end we show that early warning indicators robustly detect critical slowing for the marine ice sheet instability. We are thereby able to identify three distinct tipping points in response to increases in ocean-induced melt. The third and final event, triggered by an ocean warming of approximately 1.2 °C from the steady state model configuration, leads to a retreat of the entire glacier that could initiate a collapse of the West Antarctic Ice Sheet.

1. Introduction

The West Antarctic Ice Sheet (WAIS) is a tipping element of the earth system (Lenton *et al.*, 2008) and its collapse, potentially driven by the Marine Ice Sheet Instability (MISI) (Feldmann and Levermann, 2015), would result in over 3m of sea level rise (Fretwell *et al.*, 2013). Key to the MISI are the conditions at the grounding line - the transition line at which the grounded ice begins to float on the ocean forming ice shelves. In steady state, ice flux across the grounding line balances the surface accumulation upstream. If a grounding line retreats over a region of bed where ice flux increases and is not balanced by a corresponding increase in accumulation, the net mass balance is negative and retreat will continue (Weertman, 1974; Schoof, 2007). Conversely, grounding line advance leading to an increasing accumulation greater than the change in flux will lead to a continued advance. In this regime, a small perturbation in forcing can result in the system crossing a tipping point, beyond which a positive feedback propels the system to a contrasting state (Fig. 1c). A complex range of factors can either cause or

https://doi.org/10.5194/tc-2020-186
Preprint. Discussion started: 4 August 2020

suppress the MISI (Haseloff, 2018; Pegler, 2018) and the difficulties in predicting this behaviour are a major source of uncertainty for future sea level rise projections (Church *et al.*, 2013; Bamber *et al.*, 2019; Oppenheimer *et al.*, in press; Robel *et al.* 2019).

One area of particular concern is the Amundsen Sea region. Pine Island (PIG) and Thwaites glaciers, the two largest glaciers in the area, are believed to be particularly vulnerable to the MISI (Favier *et al.*, 2014; Rignot *et al.*, 2014). Palaeo and observational records of PIG show a history of retreat, driven by both natural and anthropogenic variability in ocean forcing (Jenkins *et al.*, 2018; Holland *et al.*, 2019). One possible MISI driven retreat might have happened when PIG unpinned from a submarine ridge in the 1940s (Jenkins *et al.*, 2010, Smith *et al.*, 2016). Recent modelling studies indicate that a larger scale MISI event may now be underway for both Pine Island and Thwaites glaciers that would lead to substantial and sustained mass loss throughout the coming centuries (Favier *et al.*, 2014, Jenkins *et al.*, 2016, Joughin *et al.*, 2010). Being able to identify a MISI driven retreat and differentiate this from an externally forced retreat where a tipping point has not been crossed is vital information for projections of future sea level rise.

This tipping behaviour of the MISI is an example of a fold (or saddle-node) bifurcation in which three equilibria exist; an upper and lower stable branch and a middle unstable branch (Fig. 1c) (Schoof, 2007). Starting on the upper stable branch, perturbing the system beyond a tipping point (x_1 in Fig. 1c) will induce a catastrophic shift to the lower and contrasting stable state. Importantly (and in contrast to a system such as that shown in Fig.1a and 1b), in order to restore conditions to the state prior to a collapse it is not sufficient to simply reverse the forcing to its previous value. Instead, the forcing must be taken back further (to point x_2), which in some cases may be far beyond the parameter space that triggered the initial collapse. This type of behaviour is known as hysteresis. A large change in response to a small forcing is not necessarily indicative of a hysteresis, as shown in Fig.1b. Tipping points are crossed in both Fig. 1c and Fig. 1d and both cases are often referred to as irreversible, although the two are distinct in that only Fig. 1d is irreversible for any change in the control parameter. Diagnosing whether or not a tipping point has been crossed without some prior knowledge of the system is not generally possible without reversing the forcing to see if a hysteresis has occurred. An alternative approach to identify tipping points is based on a process known as *critical slowing*, which is known to precede fold bifurcations of this type (Wissel, 1984; van Nes and Scheffer, 2007; Davos *et al.*, 2008; Scheffer *et al.*, 2009). Critical slowing is a general feature of non-linear systems and refers to an increase in the time a system takes to recover from perturbations as a tipping point is approached (Wissel, 1984). We will explore both hysteresis and critical slowing as indicators of tipping points in our model simulations.

Here, we map out the stability regime of Pine Island Glacier using numerical model simulations. We force the model with a slowly increasing ocean melt rate and identify three periods of rapid retreat with the methodology explained in Sect. 2.1. Using statistical tools from dynamical systems theory, introduced in Sect. 2.2, we find critical slowing preceding each of these retreat

https://doi.org/10.5194/tc-2020-186
Preprint. Discussion started: 4 August 2020

events and go on to demonstrate that these are indeed tipping points in Sect. 3. This is confirmed by analysing the hysteresis behaviour of the glacier, showing the existence of unstable grounding line positions. To our knowledge, this is the first time that the stability regime of Pine Island Glacier has been investigated in this detail and the first time that tipping point indicators have been applied to ice sheet model simulations. Our results reveal the existence of multiple smaller tipping points that when crossed could easily be mis-identified as simply periods of rapid retreat, with the irreversible and the self-sustained aspect of the retreat being missed.

2. Methods

We conduct a quasi-steady modelling experiment whereby we subject PIG to slowly increasing rates of basal melt underneath its adjacent ice shelf (Fig. 2). We differentiate between these simulations and simulations run to a true steady state, discussed later, in which the melt rate is held at a constant value and the simulation continues until the change in ice volume is approximately equal to zero. Quasi-steady state experiments have previously been successfully applied to identify the tipping point of the Greenland Ice Sheet with respect to the melt-elevation feedback (Robinson *et al.*, 2012). We use basal melt rate as the control parameter, since erosion of ice shelves by the intrusion of warm ocean currents is widely accepted as the mechanism responsible for the considerable changes currently observed in this region (Shepherd *et al.*, 2004, Rignot *et al.*, 2014; Rignot 1998; Joughin *et al.*, 2010; Park *et al.*, 2013, Gudmundsson *et al.*, 2019). Sub-ice-shelf melt rates are increased linearly from a value that generates a steady state for the present-day glacier configuration. Based on the numerical experiments we then evaluate early warning indicators to test for critical slowing.

2.1 Model description

All simulations use the community Úa ice-flow model (Gudmundsson *et al.*, 2012; Gudmundsson 2013, Gudmundsson 2020), which solves the dynamical equations for ice flow in the shallow ice stream approximation (SSTREAM or SSA) (Hutter, 1983). Bedrock geometry for the Pine Island Glacier domain is a combination of the R-Topo2 dataset (Schaffer *et al.*, 2016) and, where available, an updated bathymetry of the Amundsen Sea Embayment (Millan *et al.*, 2014). Surface ice topography is from CryoSat-2 altimetry (Slater *et al.*, 2018). Depth-averaged ice density is calculated using a meteoric ice density of 917 kg m^{-3} together with firn depths obtained from the RACMO2.1 firn densification model (Ligtenberg *et al.*, 2011). Snow accumulation is a climatological record obtained from RACMO2.1 (Lenaerts *et al.*, 2012).

Viscous ice deformation is described by the Glen Steineman flow law $\dot{\varepsilon} = A\tau_E^n$ with exponent $n = 3$ and basal motion is modelled using a Weertman sliding law $u_b = C{\tau_b}^m$ with exponent $m = 3$. Rheology and sliding use spatially varying parameters for the ice rate factor (A) and basal slipperiness(C), respectively, to initialise the model with present day ice velocities. These are obtained via inverse methods using satellite observations of surface ice velocity from the Landsat 8 dataset (Scambos *et al.* 2016; Fahnestock *et al.* 2016). An optimal solution is obtained by minimising a cost function that includes

https://doi.org/10.5194/tc-2020-186
Preprint. Discussion started: 4 August 2020

both the misfit between observed and modelled velocities and regularisation terms, to avoid overfitting. An additional term in the cost function penalises initial changes in ice thickness in order to avoid large transients at the start of simulations. This approach helps to provide a steady-state configuration of PIG from which we can conduct our perturbation experiments.

The Úa model solves the system of equations with the finite element method on an unstructured mesh, generated with mesh2d (Engwirda *et al.* 2014). The mesh remains fixed throughout the simulation to avoid contaminating the time series with errors resulting from remapping fields onto a new mesh. The mesh is refined in regions of high strain rate gradients, fast ice flow and around the grounding line. The region of grounding line mesh refinement, in which the average element size is ~750m, extends upstream sufficiently far so that the grounding line always remains within this region until after the final MISI collapse.

Basal melt rates are calculated using a widely used, local quadratic dependency on thermal forcing:

$$M = f\gamma_T \left(\frac{\rho_w c_p}{\rho_i L_i}\right)^2 (T_0 - T_f)|T_0 - T_f|,$$

where γ_T is the constant heat exchange velocity, ρ_w is sea water density, c_p is the specific heat capacity of water, ρ_i is ice density, L_i is the latent heat of fusion of ice, T_0 is the thermal forcing and T_f is the freezing temperature (Favier *et al.* 2019). The initial melt rate factor (f) is chosen such that the model finds a steady state with a grounding line approximately coincident with its position as given in Bedmap2 (Fretwell *et al.* 2013). This melt rate factor forms the control parameter for our Pine Island simulations and is increased linearly to drive the region to collapse. The statistical methods outlined below rely on extracting the time it takes for the system to return to a steady state after small perturbations (referred to hereafter as the recovery time). We therefore add a synthetic melt rate variability to our linearly increasing forcing, generated as a surrogate time series of an Amundsen Sea ocean temperature proxy (Jenkins *et al.* 2018). As shown in more detail below, this ensures that the system response contains sufficient variability to extract information about critical slowing and thereby facilitating the calculation of early warning indicators.

2.2 Critical slowing and early warning indicators

As complex systems approach a tipping point, they show early warning signals which can allow us to anticipate or even predict the onset of a tipping event (Wissel, 1984). Evidence of these early warnings have been found to precede, for example, collapse of the thermohaline circulation (Held and Kleinen, 20014; Lenton, 2011), onset of epileptic seizures (Litt, 2001; McSharry and Tarassenko, 2003), crashes in financial markets (May *et al.*, 2008, Diks *et al.*, 2018), onset of glacial terminations (Lenton, 2011) and wildlife population collapses (Scheffer *et al.*, 2001). Critical slowing is one example of an early warning signal that has been used extensively in various studies of this kind. Using this approach to detect a MISI event is first validated with an idealised flowline setup of a marine ice sheet, in which we determine the change in recovery time before a tipping point directly through multiple stepwise perturbations of the control parameter (Appendix A). Identifying critical slowing in this way is straightforward but is not practical for a realistic model forcing which would not normally take the form of a step function. A

https://doi.org/10.5194/tc-2020-186
Preprint. Discussion started: 4 August 2020

more general approach, which we adopt for our simulation of PIG, is to analyse the recovery time of the system as it is forced with natural variability using statistical tools.

A first decision to make is what quantity to measure in order to look for critical slowing in our model simulations and there are a number of possible options. One choice could be changes in ice volume, since it can be related to sea level rise and ice sheet model simulations tend to focus on this result. However ice volume varies very smoothly over time, making it difficult to detect changes in the system recovery time. Instead, we use the integrated grounding line flux, which shows much more variability and whose change is directly related to the MISI mechanism. Prior to the calculation of critical slowing indicators, the model output is aggregated to remove short term 'weather noise' and detrended to remove nonstationarities (detrending is included in the Detrended Fluctuation Analysis (DFA) algorithm and therefore not required before calculation of the DFA indicator). Detrending was done using a Gaussian kernel smoothing function that has been shown to perform better than linear detrending (Lenton *et al.* 2012). A smoothing bandwidth was selected that removed long term trends without overfitting the model time series. Indicators are calculated over a moving window with a length of 300 years.

From the processed time series, we calculate three different early warning indicators:

1. Critical slowing is measurable as an increase in the state variable auto-correlation. We measure this here using the lag-1 auto-correlation function (Dakos *et al.*, 2008; Scheffer *et al.*, 2009; Held and Kleinen, 2004) applied to the grounding line flux over a 300 year moving window preceding each tipping point (hereafter referred to as the ACF indicator).
2. Similarly, detrended fluctuation analysis (Peng *et al.*, 1994) (hereafter referred to as the DFA indicator) measures increasing auto-correlation in a time series and we apply this with the same moving window approach.
3. An additional consequence of critical slowing is that variance will increase as a tipping point is approached (Scheffer *et al.*, 2009). We calculate variance of grounding line flux for each moving window and this can be used in conjunction with other indicators to increase robustness.

Two different criteria are frequently used to assess early warning indicators and determine whether a tipping point is being approached. The first is simply to determine whether or not an indicator increases in the run up to a tipping event. This is often measured by calculating the nonparametric Kendall's τ coefficient, which equals one if the indicator is monotonically increasing with time (Dakos *et al.* 2008; Kendall, 1948). A second criteria is whether the indicators reach a critical value (in both cases a value of one) at the onset of the tipping event and thus can be used to predict when that event will happen. The second is clearly more useful but often fails in high complexity models. This failure can be a result of variability in the control variable pushing the system over a tipping point despite its long-term mean being far from its critical value.

https://doi.org/10.5194/tc-2020-186
Preprint. Discussion started: 4 August 2020

3. Results

The quasi-equilibrium simulation shows three potential tipping points with respect to the applied melt (Fig. 3). Upon crossing each threshold, indicated by the numbered blue dots in Fig. 3, PIG undergoes periods of not only rapid but (as we show later) also self-sustained and irreversible mass loss. At this stage, relying only on a record of changes in ice volume resulting from an increasing forcing (solid black line in Fig. 3), one can only speculate that these are indeed tipping points and more analysis is necessary to confirm this hypothesis, as we go on to later. The last of the three events causes an irreversible collapse within the entire model domain (Fig 3a). We increase basal melt rates gradually and in a quasi-steady-state manner to ensure that successive retreat events can be isolated and their effects do not overlap during the simulation. A more rapidly increasing forcing could lead to one tipping point cascading into the next and result in three individual tipping points being misinterpreted as only one event. Grounding line positions before each of these retreat events and after the final collapse are shown in Fig. 2. Events 1 and 2 each contribute approximately 20mm of sea-level rise while event 3, which arises after slightly more than doubling current melt rates, contributes approximately 100mm. The actual sea level rise that would result from this third and largest event is likely to be larger since in our simulation the effects stop at the domain boundary and in reality neighbouring drainage basins would be affected.

3.1 Early warning for the marine ice sheet instability

The three periods of MISI-driven retreat after a tipping point has been crossed can be identified clearly using early warning indicators (Fig. 4). The ACF early warning indicator increases and tends to one as the tipping points are approached (Fig. 4a-c), indicating a tendency to an infinitely long recovery time as predicted by theory (Wissel, 1984). We calculate Kendall's τ coefficient to identify trends in the indicator, with a value of one representing a monotonic increase in the indicator with time (SI). The positive Kendall's τ coefficient shows that in all three cases, the lag-1 auto-correlation increases before the onset of unstable retreat. Furthermore, the indicator reaches a critical value relatively close in time to when the MISI event gets underway.

These findings are supported by the DFA indicator. For this early warning indicator, a scaling exponent is calculated that reaches a critical value at 1.5, equivalent to a random walk (rescaled here to reach a critical value at unity to aid comparison with the ACF indicator) (Livina and Lenton, 2007). Also here, the Kendall's τ coefficient indicates a significant increase of the indicator when approaching the tipping points. We show the change in normalised variance calculated over each time window and in all cases this increases ahead of the tipping points being crossed with a positive Kendall's τ coefficient. The increase in variance gives greater confidence to the findings of the other two early warning indicators that a tipping point is being crossed, although variance cannot be used directly to predict when that threshold will be crossed.

https://doi.org/10.5194/tc-2020-186
Preprint. Discussion started: 4 August 2020

3.2 Hysteresis of Pine Island Glacier

In order to verify that we have correctly identified tipping points using the early-warning indicators, we run the model to steady state for a given melt rate to search for hysteresis loops that indicate the presence of unstable grounding line positions. These simulations start from either the initial model setup (advance steady state) or the configuration just prior to the final tipping point (retreat steady state) and the model is run for a range of fixed melt rate until it reaches a steady state. The first two tipping events show relatively small but clearly identifiable hysteresis loops (Fig. 3b), for which recovery of the grounding line position requires reversing the forcing beyond the point at which retreat was triggered (i.e. as shown in Fig. 1c). The third event marks the onset of an almost complete collapse of PIG (Fig. 3a). Unlike the previous two, this collapse cannot be reversed to regrow the glacier for any value of the control parameter. This is an example of an irreversible tipping point, as shown in Fig. 1d.

3.3 Robustness of the indicators

We carry out several tests to assess the robustness of the early warning indicators, see Appendix B and C. Varying parameter choices in the time series processing steps can in some cases reduce the strength of the positive Kendall's τ correlation before each tipping point, but in general the trends are consistent and not dependant on the selected parameters (Fig. B1). A window size of 300 years is the smallest for which we find that the early warning indicators can provide a useful prediction for when a tipping point will occur (Fig. B2). Larger window sizes lead to a steadily reducing positive Kendall's τ correlation as a larger proportion of the time series is far away from a tipping event. To test whether the observed Kendall's τ correlations could have been obtained by chance we generate randomised surrogates of the model time series, process them in the same way and calculate Kendall's τ correlations. In this framework, the likelihood of obtaining our trend statistics by chance is estimated by the proportion of surrogate time series with a larger Kendall τ value than detected in the original data. We find that individually the DFA and ACF indicators are significant at the 10% level in all but one case and the significance of obtaining such positive trends for all three indicators at the same time is significant at the 1% level or less for all three MISI events (Table C1).

The indicators we have tested provide early warning of tipping points as they are approached in our transient simulation with gradually increasing melt rates. It is important to clearly understand what critical threshold is identified by the early warning indicators. In Fig. 3 the simulated steady-states show the crossing of the tipping point earlier than identified by the indicators in the transient simulation. Since the time-scales of ice are longer than the forcing time-scale, the ice-sheet system modelled here does not evolve along the steady-state branch (as shown schematically in Fig. 1c). Relaxation to a steady-state takes centuries to millennia in the simulations. This means that while technically the critical value of the control parameter (basal melt rate) might have already been crossed, the glacier state could still be reverted in the transient simulation at that point, if the basal melt rate was reduced below the critical threshold. This is true until the system state variable crosses its critical value (point x_t in Fig. 1c) – and this is the point picked up by the early warning indicators. This complication in interpreting early warning indicators is inherent to ice dynamics because of its long response time scales.

https://doi.org/10.5194/tc-2020-186
Preprint. Discussion started: 4 August 2020

4. Conclusions

Conducting quasi-steady numerical experiments, whereby the underside of the PIG ice shelf is forced with a slowly increasing ocean-induced melt, we have established the existence of three distinct tipping points. Crossing each tipping point initiates periods of irreversible and self-sustained retreat of the grounding line (MISI) with significant contributions to global sea level rise. The tipping points are identified through *critical slowing*, a general behavioural characteristic of non-linear systems as they approach a tipping point. Early warning indicators have been successfully applied to detect critical slowing in other complex systems. We here show that they robustly detect the onset of the marine ice sheet instability in the simulations of the realistic PIG configuration which is promising for application of early warning to further cryospheric systems and beyond. While the possibility of PIG undergoing unstable retreat has been raised and discussed previously, this is to our knowledge the first time the stability regime of PIG has been mapped out in this fashion. The first and second tipping events are relatively small and could be missed without careful analysis of model results but nevertheless are important in that they lead to considerable sea level rise and would require a large reversal in ocean conditions to recover from. The third and final tipping point is crossed with an increase in sub-shelf melt rates equivalent to a +1.2°C change in ocean temperatures and leads to a complete collapse of PIG. Long-term warming and shoaling trends in Circumpolar Deep Water (Holland *et al.*, 2019), in combination with changing wind patterns in the Amundsen Sea (Turner *et al.*, 2017), can expose the PIG Ice Shelf to warmer waters for longer periods of time, and make temperature changes of this magnitude increasingly likely.

Appendix A: Flowline experiments

The MISI has been a major focus of modelling efforts within the glaciological community in recent years. In an effort to assess how ice-flow models capture this behaviour, a model inter-comparison experiment was performed to calculate the hysteresis loop of advance and retreat of a marine ice sheet on a retrograde slope, known as MISMIP experiment 3 (referred to as EXP 3 hereafter, Pattyn *et al.*, 2012). As a first step to establishing whether critical slowing can be observed prior to the MISI, we undertook a slightly modified version of this experiment using the Úa ice-flow model (Gudmundsson 2012, Gudmundsson 2013, see methods). In our modified experiment, the marine ice sheet is forced towards tipping points through step perturbations in the control parameter as before, but with smaller steps and the additional constraint that the model must be in steady state after each perturbation before moving onto the next. In this experiment the chosen control parameter is the ice rate factor, a parameter linked to ice viscosity and temperature.

Following each perturbation in the ice rate factor, we analyse the e-folding relaxation time (T_R) of the state variable (in this case, grounding line position) to directly extract the recovery time of the model as it approaches each tipping point (both advance and retreat). Theory predicts that $T_R \to \infty$ close to a tipping point and that the point at which ${T_R}^{-2}$ (as plotted versus the control parameter) reaches 0 thus identifies the critical value of the control parameter, beyond which a tipping point is crossed (Wissel 1984). We show this plot for both the advance and retreat scenarios of EXP 3 in Fig. A1. In both cases the

https://doi.org/10.5194/tc-2020-186
Preprint. Discussion started: 4 August 2020

relaxation time decreases as predicted by theory, even far from the tipping point. A linear fit through the last six perturbations yields a good agreement with theory and accurately predicts the critical value of the control parameter when compared to the analytical solution (red arrows in Fig. A1) given by Schoof (2007). Critical slowing still occurs outside of this range (equivalent to a change in ice temperature of >5 °C) but using these more distant points to forecast the tipping point would yield a less accurate prediction. These results therefore provide some insight into how far from the basin of attraction we can expect the predicted linear response.

Appendix B: Indicator sensitivity

Before calculating the ACF and DFA indicators, the model output grounding line flux was processed, as described in the methods. Two parameters in this processing step are the bin size into which data are aggregated and the bandwidth of the smoothing kernel that removes long term trends in the time series. In order to check that the increasing trends in our indicators are a robust feature of our results, regardless of these choices, we conducted a sensitivity analysis. The parameters were varied by +/- 50% and the indicators were recalculated for each resulting time series. As before, we assess the utility of an indicator by whether it shows an increasing trend before each tipping point, as measured by a positive Kendall's τ coefficient. The results of this sensitivity analysis are presented for each MISI event in Fig. B1. Kendall's τ coefficient is positive for all tested combinations of parameters and all MISI events, although MISI event 2 is particularly insensitive to these parameter choices whereas the spread in Kendall's τ coefficient is greater for the other two events.

In general, critical slowing will only occur close to a tipping point. Determining how close to a tipping point a system must be in order to anticipate the approaching critical transition, i.e. the prediction radius, is an important question and also informs the selection of palaeo-records that could be used to detect an upcoming MISI event. We show results for a window size of 300 years (i.e. a record length of 600 years), which is the shortest window size for which the DFA indicator provides an accurate prediction for all tipping events. We explored the prediction radius of our model by calculating Kendall's τ for the ACF and DFA indicators and the variance for a range of window lengths, see Fig. B2. For the main tipping event, preceded by the longest stable period, the indicators gradually lose their ability to anticipate a tipping event as more data is included further from the event. The same is true for the two smaller tipping events, but the drop off is quicker such that the indicators break down for window lengths > 500 years. These results suggest that the prediction radius is relatively small and window sizes that are too large, and hence include data far from a tipping point, lose their ability to serve as early-warning indicators.

https://doi.org/10.5194/tc-2020-186
Preprint. Discussion started: 4 August 2020

Appendix C: Indicator significance

In addition to a sensitivity analysis, it is important to check that trends in the calculated indicators are statistically significant and not the result of random fluctuations. We follow the method originally proposed by Dakos *et al.* (2012) and produce surrogate datasets from the model time series that have many of the same properties but should not contain any critical slowing trends. We generate 1000 of these datasets using an autoregressive AR(1) process based surrogate. For each of these datasets we calculate the ACF and DFA indicators and variance in the same way as with the model time series and then estimate the trend with values of Kendall's τ coefficient. We calculate the probability of our results being a result of chance for each indicator and for all three combined as the proportion of cases for which the surrogate dataset was found to have a higher correlation than the model time series. We find that $P<0.1$ in all but one instance for the ACF and DFA indicators but variance trends were generally less significant (Table C1). However, the combined probability that all three indicators would be equally positive as a result of chance was less than 0.02 for the first MISI event and less than 0.005 for the second two events.

Code availability

The source code of the Úa ice-flow model is available from https://github.com/ghilmarg/UaSource (last access: 30 June 2020) and raw model output is available from the authors upon request.

Author contribution

SHRR and RR conceived the study, SHRR conducted the modelling experiments, JFD contributed to the statistical analysis and surrogate time series, JDR provided an initial model setup. SHRR and RR wrote the manuscript with contributions from all authors.

Competing interests

The authors declare that they have no conflict of interest.

References

Bamber, J. L., Oppenheimer, M., Kopp, R. E., Aspinall, W. P., Cooke, R. M. Ice sheet contributions to future sea-level rise from structured expert judgment. *Proceedings of the National Academy of Sciences*, **116 (23),** 11195-11200 https://doi.org/10.1073/pnas.1817205116, (2019)

Church, J. A. *et al.* in *Climate Change 2013: The Physical Science Basis. Contribution of Working Group I to the Fifth Assessment Report of the Intergovernmental Panel on Climate Change* (eds Stocker, T. F. *et al.*) Ch. 13, 1137–1216 (Cambridge Univ. Press, 2013)

Dakos *et al.* Slowing down as an early warning signal for abrupt climate change, *Proceedings of the National Academy of Sciences,* **105 (38),** 14308-14312, https://doi.org/10.1073/pnas.0802430105, (2008)

Diks, C., Hommes, C., and Wang, J.: Critical slowing down as an early warning signal for financial crises?, *Empirical Economics*, https://doi.org/10.1007/s00181-018-1527-3, (2018)

Dutrieux, P. *et al.*: Strong sensitivity of Pine Island ice-shelf melting to climatic variability. *Science*, **343,** 174-178. 10.1126/science.1244341, (2014)

Engwirda, D.: Locally-optimal Delaunay-refinement and optimisation-based mesh generation, Ph.D. Thesis, *School of Mathematics and Statistics, The University of Sydney,* September, (2014)

Fahnestock, M., Scambos, T., Moon, T., Gardner, A., Haran, T., and Klinger, M.: Rapid large-area mapping of ice flow using Landsat 8, *Remote Sens. Environ.*, **185**, 84–94, https://doi.org/10.1016/j.rse.2015.11.023, (2016)

Favier *et al.* Retreat of Pine Island Glacier controlled by marine ice-sheet instability. *Nature Climate Change*, **4,** 117-121. https://doi.org/10.1038/nclimate2094, (2014)

Favier, L., Jourdain, N. C., Jenkins, A., Merino, N., Durand, G., Gagliardini, O., Gillet-Chaulet, F., and Mathiot, P.: Assessment of sub-shelf melting parameterisations using the ocean–ice-sheet coupled model NEMO(v3.6)–Elmer/Ice(v8.3) , *Geosci. Model Dev.*, **12**, 2255–2283, https://doi.org/10.5194/gmd-12-2255-2019, (2019)

Feldmann, J. and Levermann, A. Collapse of the West Antarctic Ice Sheet after local destabilization of the Amundsen Basin, *Proceedings of the National Academy of Sciences*, 112 (46), 14191-14196, https://doi.org/10.1073/pnas.1512482112, (2015)

Fretwell, P. et al.: Bedmap2: improved ice bed, surface and thickness datasets for Antarctica, *The Cryosphere*, **7,** 375–393, https://doi.org/10.5194/tc-7-375-2013, (2013)

Gudmundsson, G. H., Krug, J., Durand, G., Favier, L., and Gagliardini, O.: The stability of grounding lines on retrograde slopes, *The Cryosphere*, **6**, 1497–1505, https://doi.org/10.5194/tc-6-1497-2012, (2012)

Gudmundsson, G. H.: Ice-shelf buttressing and the stability of marine ice sheets, *The Cryosphere*, **7**, 647–655, https://doi.org/10.5194/tc-7-647-2013, (2013)

Gudmundsson, G. H., Paolo, F. S., Adusumilli, S., and Fricker, H. A. Instantaneous Antarctic ice- sheet mass loss driven by thinning ice shelves. *Geophysical Research Letters*, 46, 13903–13909. https://doi.org/10.1029/2019GL085027, (2019)

Gudmundsson, G. H. GHilmarG/UaSource: Ua2019b (Version v2019b). doi: 10.5281/zenodo.3706624 (2020)

Haseloff, M., and Sergienko, O.: The effect of buttressing on grounding line dynamics. *Journal of Glaciology*, **64**(245), 417-431. doi:10.1017/jog.2018.30 (2018)

Held, H. and Kleinen, T.: Detection of climate system bifurcations by degenerate fingerprinting, *Geophysical Research Letters*, **31**, 1–4, https://doi.org/10.1029/2004GL020972, (2004)

Holland, P. R., Bracegirdle, T. J., Dutrieux, P., Jenkins, A. and Steig, E. J.: West Antarctic ice loss influenced by internal climate variability and anthropogenic forcing. *Nature Geoscience*, **12**. 718-724. 10.1038/s41561-019-0420-9, (2019)
Jenkins, A. *et al.* Decadal Ocean Forcing and Antarctic Ice Sheet Response: Lessons from the Amundsen Sea. *Oceanography*, **29,** 106-117. https://doi.org/10.5670/oceanog.2016.103, (2016)

Hutter, K.: Theoretical Glaciology, D. Reidel, Dordrecht, Netherlands. (1983)

Jenkins, A. *et al.*: West Antarctic Ice Sheet retreat in the Amundsen Sea driven by decadal oceanic variability, *Nature Geoscience*, **11**, 733–738, https://doi.org/10.1038/s41561-018-0207, (2018)

Jenkins, A., Dutrieux, P., Jacobs, S. *et al.* Observations beneath Pine Island Glacier in West Antarctica and implications for its retreat. *Nature Geosci* **3,** 468–472, https://doi.org/10.1038/ngeo890, (2010)

Joughin, I., Smith, B. E., & Holland, D. M.: Sensitivity of 21st century sea level to ocean-induced thinning of Pine Island Glacier, Antarctica, *Geophysical Research Letters*, **37**, https://doi.org/10.1029/2010GL044819 (2010)

Kendall, M. G.: Rank correlation methods, Oxford, Griffen, (1948)

Lenaerts, J. T. M., van den Broeke, M. R., van de berg, W. J., van Mejigaard, E., Kuipers Munneke, P.: A new, high-resolution surface mass balance map of Antarctica (1979-2010) based on regional atmospheric climate modeling. *Geophys. Res. Lett.*, **39**, L04501, doi:10.1029/2011GL050713, (2012)

Lenton, T. M. *et al.*: Tipping elements in the Earth's climate system, *Proceedings of the National Academy of Sciences*, **105 (6),** 1786-1793, https://doi.org/10.1073/pnas.0705414105, (2008)

Lenton, T. M.: Early warning of climate tipping points, *Nature Climate Change*, **1**, 201–209, https://doi.org/10.1038/nclimate1143, (2011)

Lenton, T. M., Livina, V. N., Dakos, V., and Scheffer, M.: Climate bifurcation during the last deglaciation?, *Climate of the Past*, **8**, 1127–1139, https://doi.org/10.5194/cp-8-1127-2012, (2012)

Ligtenberg, S. R. M., Helsen, M. M., van den Broeke, M. R.:An improved semi-empirical model for the densification of Antarctic firn. The Cryosphere, 5, 809-819, doi: doi:10.5194/tc-5-809-2011, (2011)

Litt, B., Esteller, R., Echauz, J., D'Alessandro, M., Shor, R., Henry, T., Pennell, P., Epstein, C., Bakay, R., Dichter, M., and Vachtsevanos, G.: Epileptic Seizures May Begin Hours in Advance of Clinical Onset: A Report of Five Patients, *Neuron*, **30**, 51–64, https://doi.org/https://doi.org/10.1016/S08966273(01)00262-8, (2001)

Livina, V. N. and Lenton, T. M.: A modified method for detecting incipient bifurcations in a dynamical system, *Geophysical Research Letters*, **34**, 1–5, https://doi.org/10.1029/2006GL028672, (2007)

May, R., Levin, S. A., and Sugihara, G.: Ecology for bankers, *Nature*, **451**, 893–895, https://doi.org/10.1038/451893a, (2008)

McSharry, P. E., A., S. L., and Tarassenko, L.: Prediction of epileptic seizures: are nonlinear methods relevant?, *Nature Medicine*, **9**, 241–242, https://doi.org/10.1038/nm0303-241, (2003)

Millan, R., Rignot, E., Bernier, V., Morlighem, M., and Dutrieux, P.: Bathymetry of the Amundsen Sea Embayment sector of West Antarctica from Operation IceBridge gravity and other data, Geophys. Res. Lett., 44, 1360– 1368, doi:10.1002/2016GL072071, (2017)

Oppenheimer, M., B.C. Glavovic , J. Hinkel, R. van de Wal, A.K. Magnan, A. Abd-Elgawad, R. Cai, M. Cifuentes-Jara, R.M. DeConto, T. Ghosh, J. Hay, F. Isla, B. Marzeion, B. Meyssignac, and Z. Sebesvari, 2019: Sea Level Rise and Implications for Low-Lying Islands, Coasts and Communities. In: *IPCC Special Report on the Ocean and Cryosphere in a Changing Climate* [H.-O. Pörtner, D.C. Roberts, V. Masson-Delmotte, P. Zhai, M. Tignor, E. Poloczanska, K. Mintenbeck, A. Alegría, M. Nicolai, A. Okem, J. Petzold, B. Rama, N.M. Weyer (eds.)]. In press.

Park, J. W., Gourmelen, N., Shepherd, A., Kim, S. W., Vaughan, D. G., and Wingham, D. J.: Sustained retreat of the Pine Island Glacier, *Geophysical Research Letters*, **40**, 2137–2142, https://doi.org/10.1002/grl.50379, (2013)

Pattyn, F. *et al.*: Results of the Marine Ice Sheet Model Intercomparison Project, MISMIP, *The Cryosphere*, **6**, 573–588, https://doi.org/10.5194/tc-6-573-2012, (2012)

Pegler, S.: Marine ice sheet dynamics: The impacts of ice-shelf buttressing. *Journal of Fluid Mechanics*, **857**, 605-647. doi:10.1017/jfm.2018.741 (2018)

Peng, C.K., Buldyrev, S. V., Havlin, S., Simons, M., Stanley, H. E., and Goldberger, A. L.: Mosaic organization of DNA nucleotides, *Phys. Rev. E*, **49**, 1685–1689, https://doi.org/10.1103/PhysRevE.49.1685, (1994)

Rignot, E. J.: Fast Recession of a West Antarctic Glacier, *Science*, **281**, 549-551, https://doi.org/10.1126/science.281.5376.549, (1998)

Rignot, E., Mouginot, J., Morlighem, M., Seroussi, H., and Scheuchl, B. Widespread, rapid grounding line retreat of Pine Island, Thwaites, Smith, and Kohler glaciers, West Antarctica, from 1992 to 2011, *Geophys. Res. Lett.*, **41,** 3502– 3509, doi:10.1002/2014GL060140, (2014)

Robel, A. A., Seroussi, H. and Roe, G. H. Marine ice sheet instability amplifies and skews uncertainty in projections of future sea-level rise, *Proc. Natl. Acad. Sci.*, **116**, 14887-14892, doi:10.1073/pnas/1904822116, (2019)

Robinson, A., Calov, R. & Ganopolski, A. Multistability and critical thresholds of the Greenland ice sheet. *Nature Clim Change* **2,** 429–432, https://doi.org/10.1038/nclimate1449, (2012)

Scambos, T., Fahnestock, M., Moon, T., Gardner, A., and Klinger, M.: Global Land Ice Velocity Extraction from Landsat 8 (GoLIVE), Version 1, NSIDC: National Snow and Ice Data Center, Boulder, Colorado USA, https://doi.org/10.7265/N5ZP442B, http://nsidc.org/data/golive, (2016)

Schaffer J, Timmermann R, Arndt JE, Kristensen SS, Mayer C, Morlighem M, et al.: A global, high-resolution data set of ice sheet topography, cavity geometry, and ocean bathymetry, *Earth System Science Data* **8**(2), 543–557, https://doi.org/10.5194/essd8-543-2016, (2016)

Scheffer, M., Carpenter, S., Foley, J. A., Folke, C. and Walker, B. Catastrophic shifts in ecosystems, *Nature*, **413,** 591-596, https://doi.org/10.1038/35098000, (2001)

Scheffer *et al.* Early-warning signals for critical transitions, *Nature*, **461,** 53-59, https://doi.org/10.1038/nature08227, (2009)

Shepherd, A., Wingham, D., and Rignot, E. Warm ocean is eroding West Antarctic Ice Sheet, *Geophys. Res. Lett.*, 31, L23402, doi:10.1029/2004GL021106, (2004)

Schoof, C. Ice sheet grounding line dynamics: Steady states, stability, and hysteresis, *J. Geophys. Res.*, **112,** F03S28, doi:10.1029/2006JF000664, (2007)

Slater, T. *et al.*: A new digital elevation model of Antarctica derived from CryoSat-2 altimetry, *The Cryosphere*, **12**, 1551–1562, https://doi.org/10.5194/tc-12-1551-2018, (2018)

Smith, J. A. *et al.* Sub-ice-shelf sediments record history of twentieth-century retreat of Pine Island Glacier, Nature, **541**, 77-80, https://doi.org/10.1038/nature20136, (2016)

Turner, J., Orr, A., Gudmundsson, G. H., Jenkins, A., Bingham, R. G., Hillenbrand, C.-D., and Bracegirdle, T. J., Atmosphere-ocean-ice interactions in the Amundsen Sea Embayment, West Antarctica, *Rev. Geophys.*, **55**, 235- 276, https://doi:10.1002/2016RG000532, (2017)

van Nes, E. H. and Scheffer, M. Slow Recovery from Perturbations as a Generic Indicator of a Nearby Catastrophic Shift, *The American Naturalist*, **169 (6),** 738-747, https://doi.org/10.1086/516845, (2007)

Weertman, J. Stability of the Junction of an Ice Sheet and an Ice Shelf. *Journal of Glaciology*, **13 (67),** 3-11. doi:10.3189/S0022143000023327, (1974)

Wissel, C.: A universal law of The characteristic return time near thresholds, *Oecologia*, **65**, 101–107, https://doi.org/10.1007/BF00384470, (1984)

https://doi.org/10.5194/tc-2020-186
Preprint. Discussion started: 4 August 2020

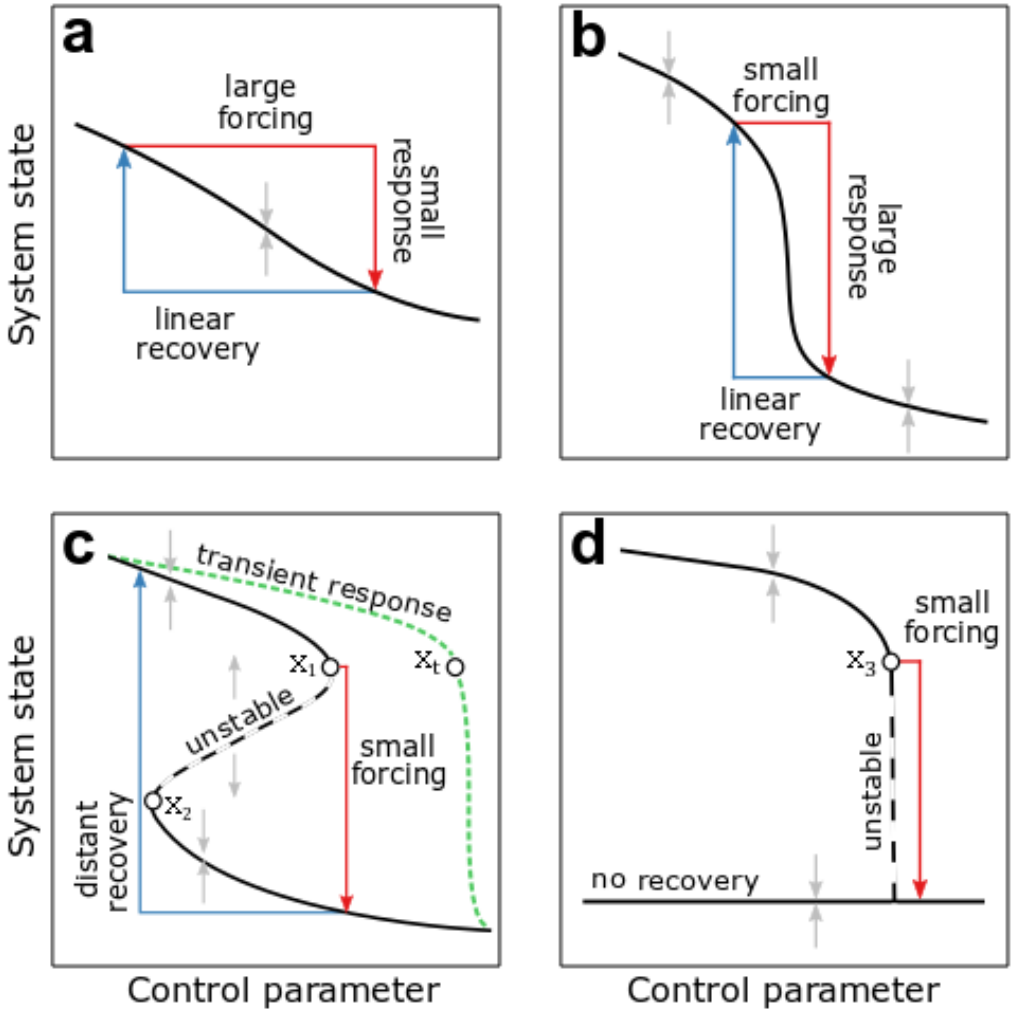

Figure 1. Possible range of behaviours for a system state (e.g. ice flux) in response to perturbations in a control parameter (e.g. ocean temperature). A system can respond to a perturbation (a) in a linear way that is directly recoverable with a reversal of the forcing, (b) with a large response to a small perturbation but that is still directly recoverable, (c) with a large response to a small perturbation that is irreversible (hysteresis behaviour), and (d) with a large response that is irreversible for any change in the control parameter. Tipping points are crossed only in panels (c) and (d) and are indicated by x1, x2 and x3. Panel (c) also shows a transient response in which the system state lags behind changes in the control parameter as is the case for ice sheets and thus crosses the irreversible system state at a later point, xt.

https://doi.org/10.5194/tc-2020-186
Preprint. Discussion started: 4 August 2020

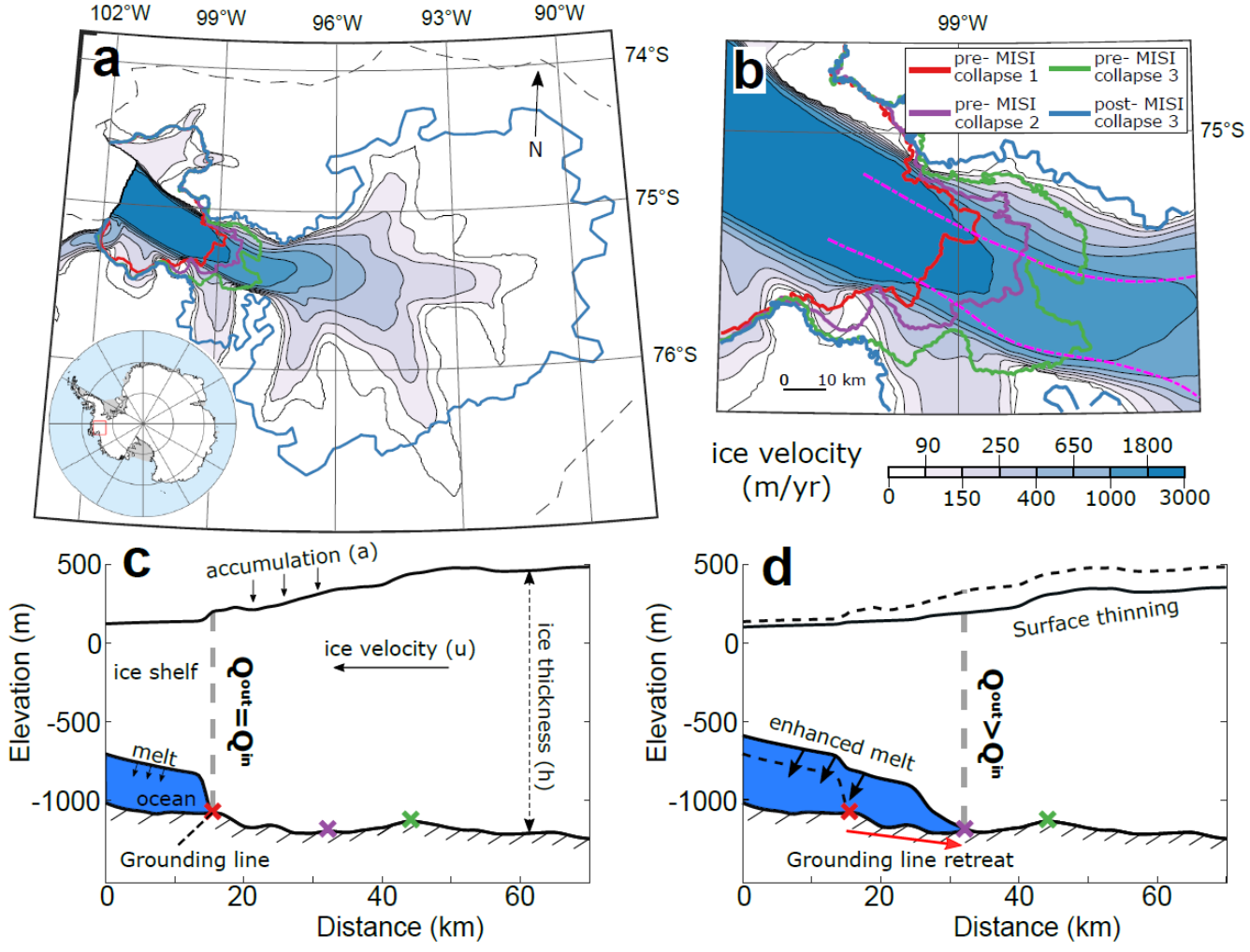

Figure 2. Marine Ice Sheet Instability events for Pine Island Glacier. Shown are (a) grounding line positions before and after the three MISI driven glacier collapses with (b) a zoom to the initial events (coloured lines). The colormap indicates initially modelled ice velocity and the model domain boundary is indicated by a dashed black contour in panel a . Panels (c) and (d) show a transect through the main trunk of PIG, calculated as an average of properties between the two dashed magenta lines in (b). The vertical section along the transect is shown (c) at the initial steady state where fluxes (Q_{in} and Q_{out}) are in balance and (d) during a MISI event where retreat causes an increase in Q_{out}, pushing the glacier to be out of balance and leading to further retreat.

https://doi.org/10.5194/tc-2020-186
Preprint. Discussion started: 4 August 2020

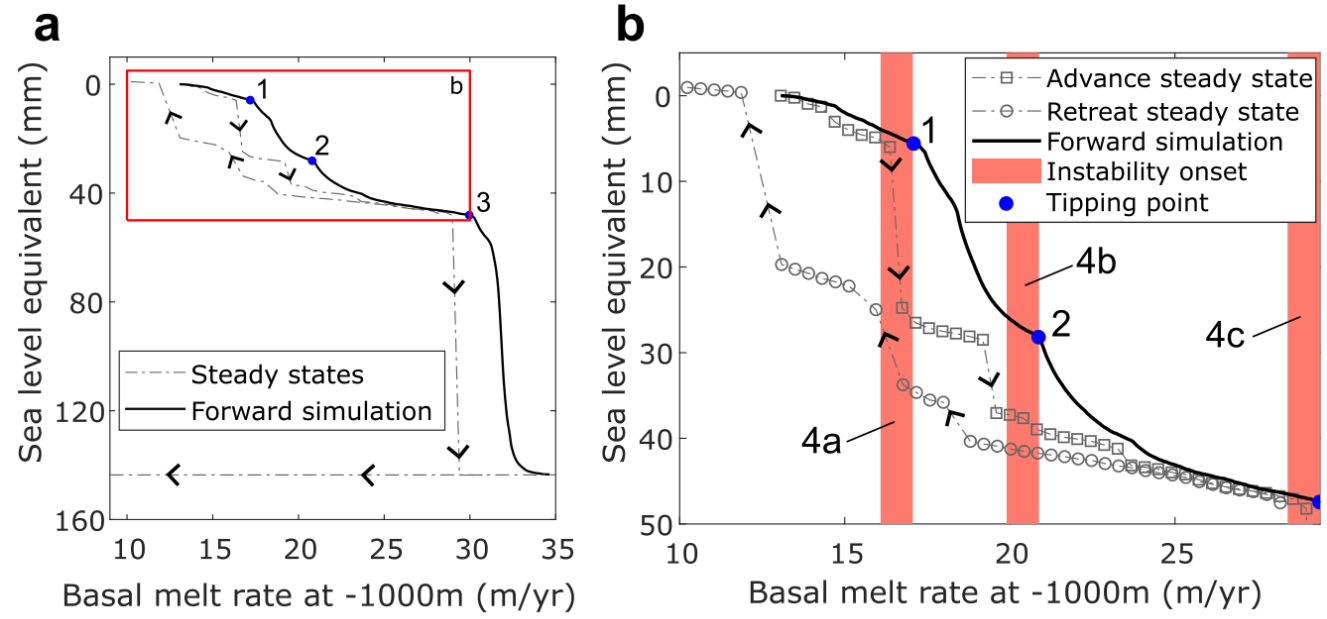

Figure 3. Change in system state in terms of sea level equivalent ice volume as a function of the control parameter, which is the melt rate at the ice-ocean interface. (a) The model is run forward with a slowly increasing basal melt rate (solid black line) and shows three distinct tipping points (blue dots). The steady states for a given melt rate in both an advance and retreat configuration are plotted as dashed grey lines, arrows indicate the direction of the hysteresis. Panel (b) focuses on the model response before the larger tipping point (event 3) and shows the three windows that we analyze for early warning indicators as shaded red boxes (Fig. 4).

https://doi.org/10.5194/tc-2020-186
Preprint. Discussion started: 4 August 2020

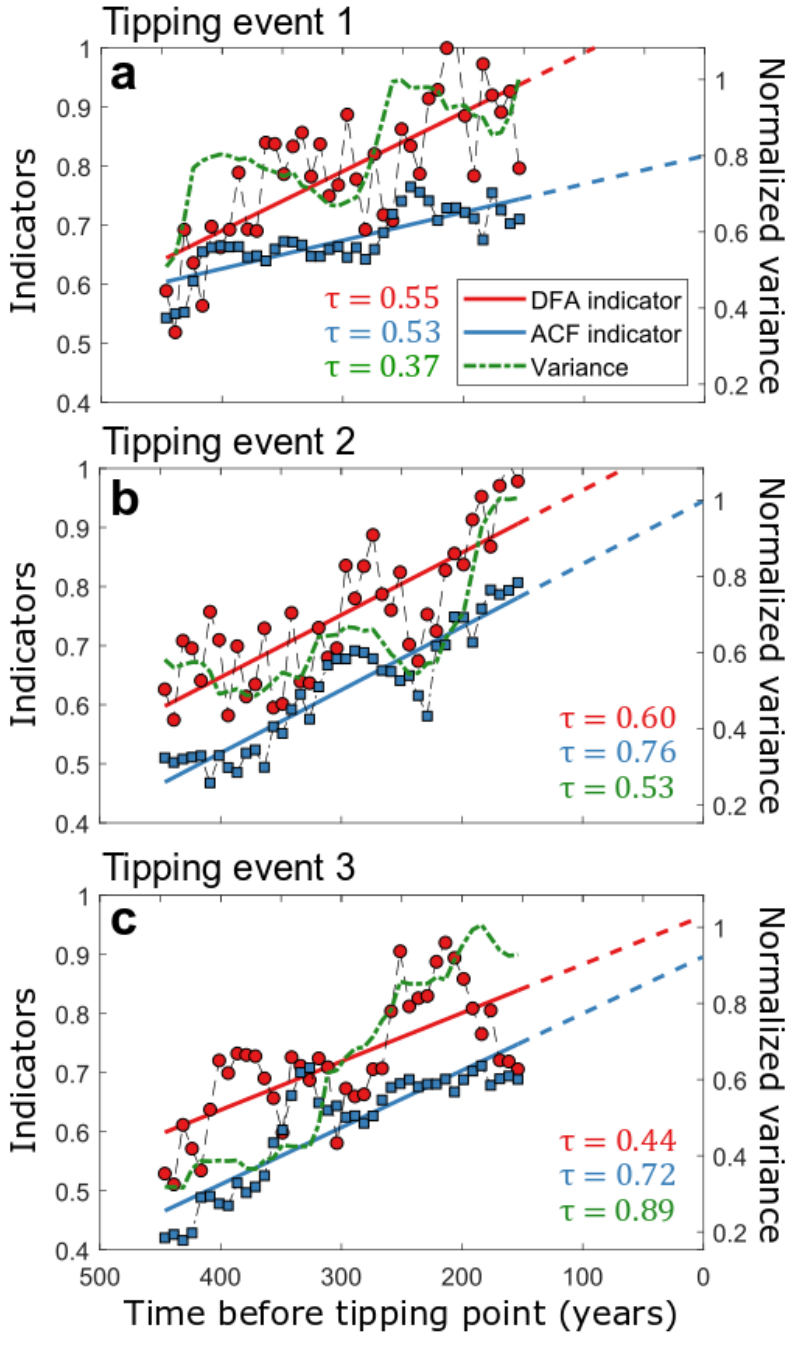

Figure 4. Early warning indicators for the marine ice sheet instability in Pine Island Glacier. Each panel shows the early warning indicators preceding each of the three MISI tipping event marked in Fig 3b, along with the linear trend extrapolated to the point in the simulation when the respective tipping event occurs. Increasing trends in all indicators are shown by a positive Kendall's τ coefficient which measures the correlation between each indicator and time between -1 and 1.

https://doi.org/10.5194/tc-2020-186
Preprint. Discussion started: 4 August 2020

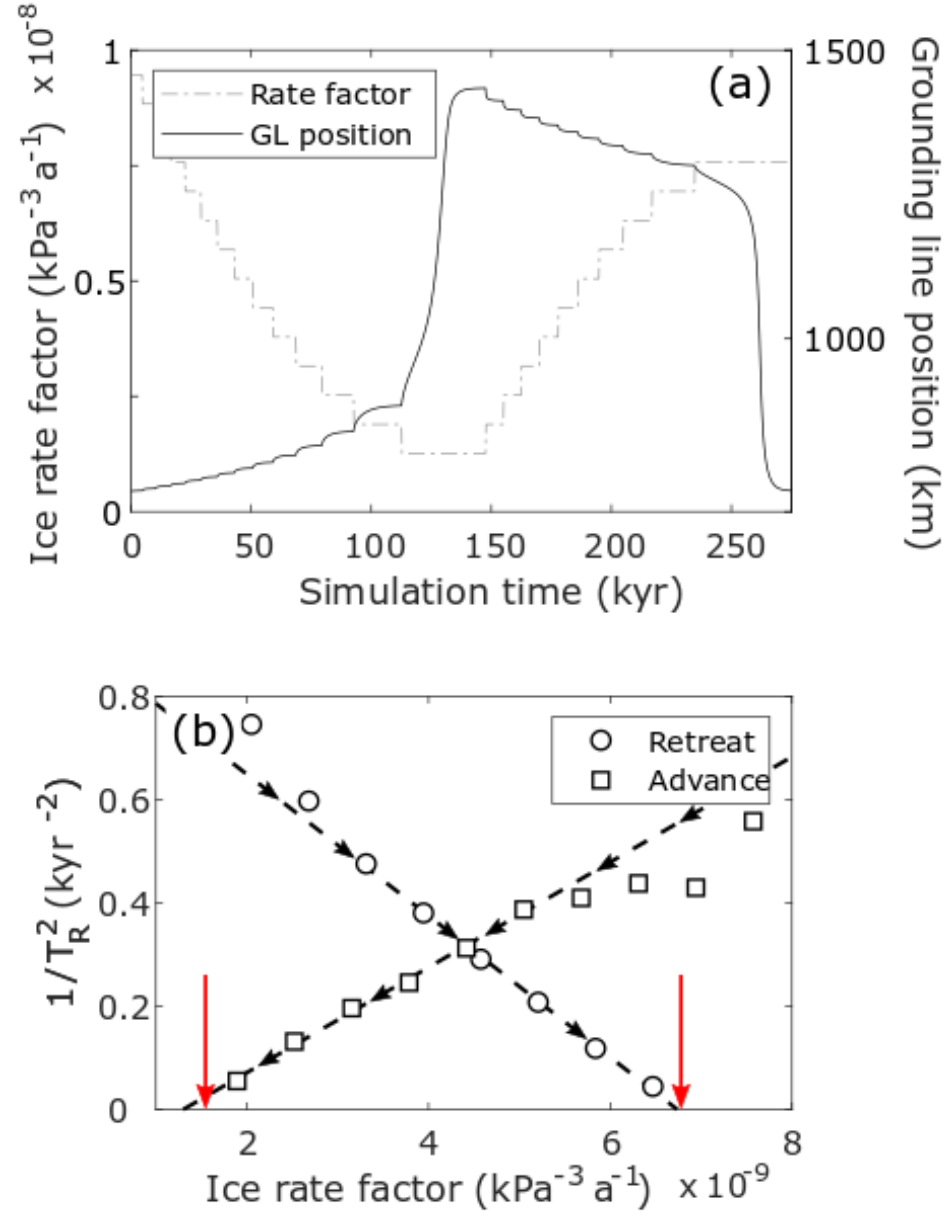

Figure A1. Results of EXP 3, showing change in GL position with time resulting from step perturbations in the ice rate factor (panel a). The calculated inverse relaxation time for each corresponding step change in rate factor in both the advance (square symbols) and retreat (circular symbols) phase is shown in panel b. The dashed line in panel b is a line of best fit, calculated for the five steps in rate factor that preceded the advance or retreat MISI phase. Red arrows indicate the rate factors for which the analytical solution predicts a MISI event and black arrows show the direction of the forcing towards each tipping point.

https://doi.org/10.5194/tc-2020-186
Preprint. Discussion started: 4 August 2020

The Cryosphere Discussions
Open Access
EGU

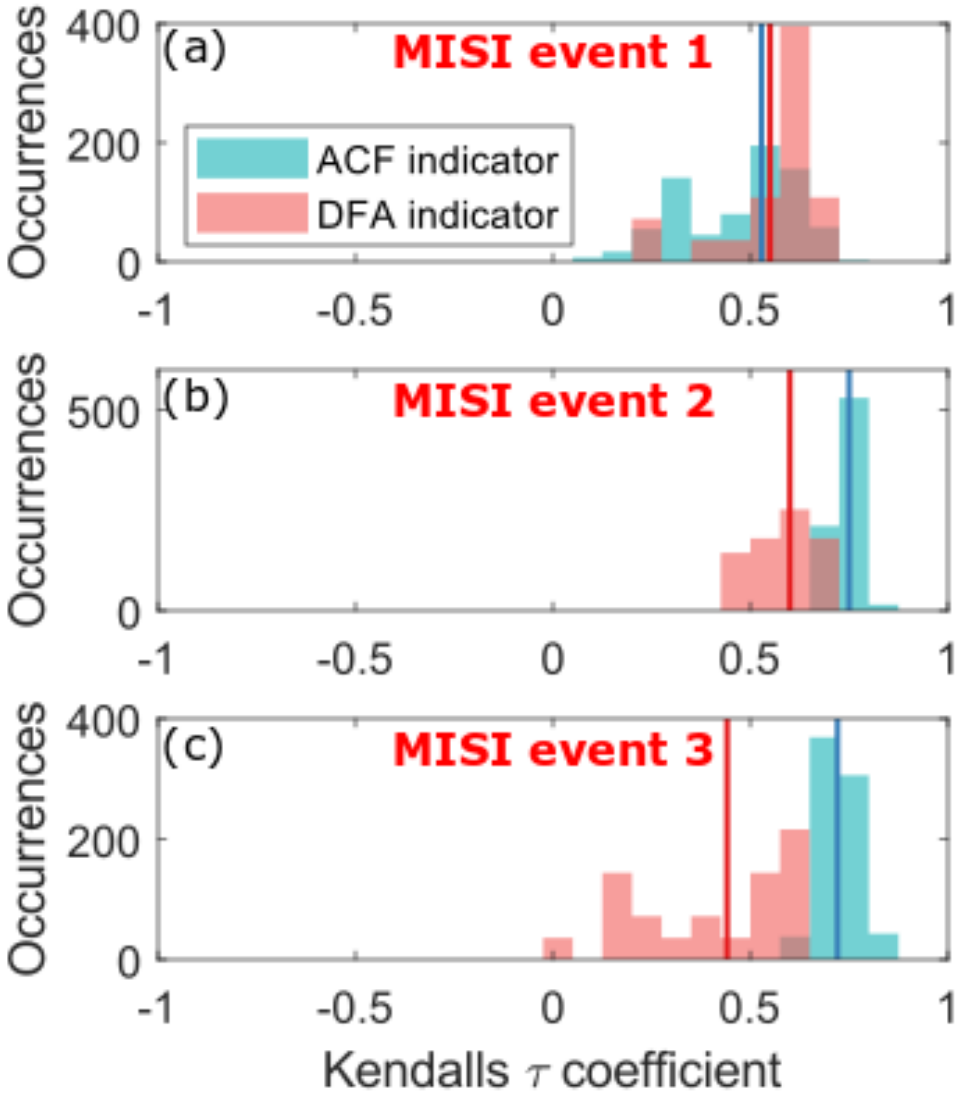

Figure B1. Sensitivity analysis for the ACF and DFA indicators. Each occurrence is the Kendall's τ coefficient for a different choice of filtering bandwidth and data aggregation. The solid red and blue lines show the Kendall's τ coefficient for the DFA and ACF indicators respectively, as calculated for the choice of parameters used in Fig. 3.

https://doi.org/10.5194/tc-2020-186
Preprint. Discussion started: 4 August 2020

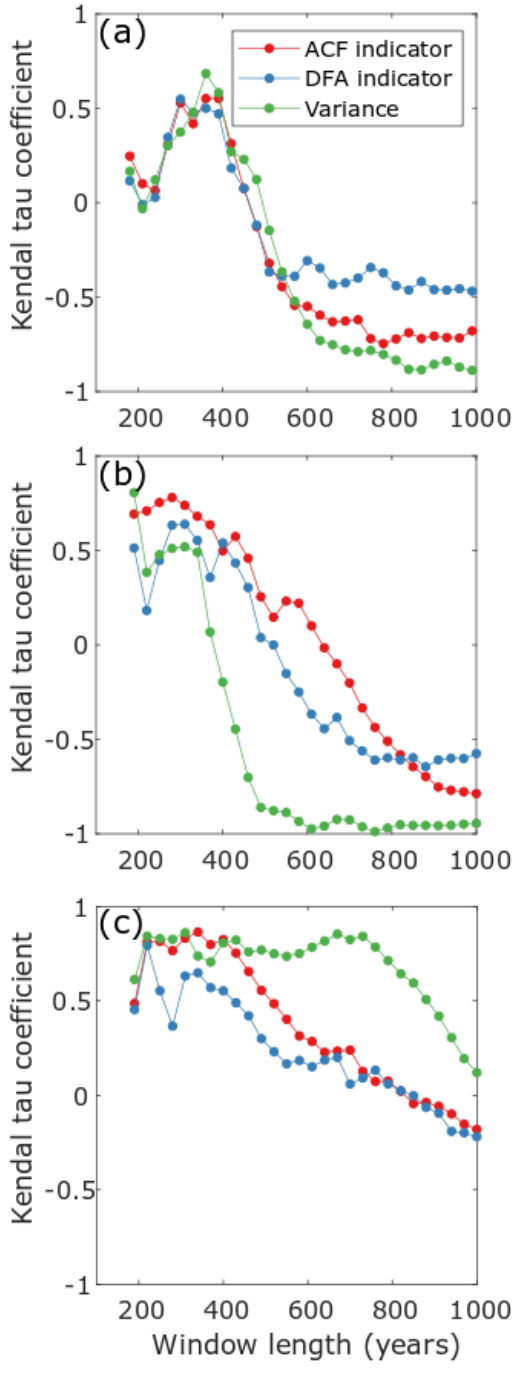

Figure B2. The effect of window length on the predictive power of early warning indicators for the MISI. The three panels show the change in Kendall's τ coefficient as calculated for each indicator versus window length for MISI events 1, 2 and 3 (panels a, b and c respectively).

https://doi.org/10.5194/tc-2020-186
Preprint. Discussion started: 4 August 2020

Event Number	Indicator name	Indicator value	Probability	Total Probability
MISI event 1	DFA	0.55	0.041	0.0198
	ACF	0.53	0.122	
	Variance	0.37	0.315	
MISI event 2	DFA	0.60	0.022	0.0030
	ACF	0.76	0.012	
	Variance	0.53	0.207	
MISI event 3	DFA	0.44	0.099	0.0044
	ACF	0.72	0.026	
	Variance	0.89	0.018	

535 **Table C1. Probability of the Kendall's τ correlation for each indicator being a result of chance. One thousand surrogate time series of the state variable are generated and the indicators and Kendall's τ correlations calculated for each one. The probability of a Kendall's τ value is then the fraction of these surrogate time series with a higher correlation coefficient. The total probability is the fraction of surrogates for which all three indicators have a higher correlation coefficient than is observed in the original model time series.**